A Novel DFT-based Scheme for PAPR Reduction in FBMC/OQAM Systems

Dejin Kong, Xing Zheng, and Tao Jiang, *Fellow, IEEE*

***Abstract*—In this letter, a novel discrete Fourier transform (DFT)-based scheme is proposed for peak to average power ratio (PAPR) reduction in filter-bank multicarrier with offset quadrature amplifier modulation (FBMC/OQAM) systems. The key idea is the combination of DFT and the concept of block repetition proposed in our previous work. Different from the conventional DFT-based PAPR reduction method, the output complex-valued signal of the DFT module is directly transmitted in the proposed DFT-based PAPR reduction method, instead of separating and transmitting the real and imaginary parts of the output signal, respectively. The proposed method can provide a solution to the low PAPR without the cost of high complexity, signal distortion or side information. To validate the performance of the proposed method, simulation results are provided in terms of complementary cumulative distribution function (CCDF) and bit error ratio (BER).**

***Index Terms*—FBMC/OQAM, PAPR, complementary cumulative distribution function, block repetition.**

I. Introduction

As one of multicarrier modulations, filter-bank multicarrier with offset quadrature amplifier modulation (FBMC/OQAM) has attracted much attention [1], [2] due to the low spectrum sidelobe. Compared with the classic orthogonal frequency division multiplexing (OFDM), the low spectrum sidelobe of FBMC/OQAM signals offers the abilities of fragmented spectrum utilization and asynchronous transmissions. Besides, better spectral efficiency can be achieved in FBMC/OQAM systems due to the absence of cyclic prefix (CP), which is usually adopted in OFDM.

However, similar to OFDM, FBMC/OQAM also suffers from the problem of high peak to average power ratio (PAPR), reducing the system spectral efficiency and energy efficiency. So far, various PAPR reduction schemes have been proposed for FBMC/OQAM systems. Two typical schemes, Partial transmit sequence (PTS) [3], [4] and selective mapping (SLM) [5]–[7] schemes, has been respectively presented for PAPR reduction in FBMC/OQAM systems, which require considerable computational complexity and side information. In [8], the authors presented a tone reservation method with sliding window for PAPR reduction, however, reservation of subcarriers results in significant loss of spectral and energy efficiencies. In [9], [10], clipping-based schemes were presented for PAPR reduction in FBMC/OQAM systems, which reduces the performances of bit error ratio (BER) and out-of-band (OOB) due to the signal distortion.

Recently, the conventional discrete Fourier transform (DFT)-based scheme was presented [11], which reduces the PAPR of FBMC/OQAM systems without the cost of high complexity, signal distortion or side information. However, due to the fact that the real and imaginary parts of the DFT output signals are separated and transmitted with a half symbol duration, the PAPR reduction is limited. Then, the improved DFT-based schemes were proposed in [12], [13], which can achieve a low PAPR at the cost of side information or computational complexity.

In this letter, we propose a novel discrete Fourier transform (DFT)-based method for PAPR reduction in FBMC/OQAM systems. The key idea is the combination of DFT and the concept of block repetition proposed in our previous work [14]. Compared with the conventional DFT-based PAPR reduction method [11], the proposed DFT-based method can achieve lower PAPR in FBMC/OQAM systems, without the cost of high complexity, signal distortion or side information.

The remainder of this paper is organized as follows. In section II, the FBMC/OQAM system and the conventional DFT-based PAPR reduction scheme are presented briefly. Section III presents the novel DFT-based PAPR reduction scheme, which is based on the the concept of block repetition proposed in our previous work in [14]. In section IV, simulation results are given and the work are concluded in section V.

II. Conventional DFT-Based PAPR Reduction Scheme in FBMC/OQAM Systems

A. System Model

For an FBMC/OQAM system with subcarriers of M as shown in Fig. 1, the equivalent baseband signal at the transmitter can be written as [15]

$$s[k] = \sum_{m=0}^{M-1} \sum_{n\in\mathbb{Z}} a_{m,n} \underbrace{g\left[k - n\frac{M}{2}\right] e^{j2\pi mk/M} e^{j\pi(m+n)/2}}_{g_{m,n}[k]}, \tag{1}$$

where $j = \sqrt{-1}$ and $g[\cdot]$ denotes the prototype filter with low spectrum sidelobe [1]. The real-valued transmitting symbol at the time-frequency position (m, n), $a_{m,n}$, is usually from the real part or imaginary part of a quadrature amplifier modulation (QAM) symbol.

Dejin Kong is with the School of Electronic and Electrical Engineering, Wuhan Textile University, Wuhan, 430074, China (e-mail: djkou@wtu.edu.cn)

Xing Zheng, Tao Jiang (corresponding author) are with the School of Electronic Information and Communications, Huazhong University of Science and Technology, Wuhan, 430074, China (e-mail: xingzheng@hust.edu.cn; tao.jiang@ieee.org)

Different from OFDM systems, the orthogonality condition is only satisfied in the real field in FBMC/OQAM systems, i.e.,

$$\Re\left\{\sum_{k=-\infty}^{\infty} g_{m,n}[k]]g^*_{m_0,n_0}[k]\right\} = \delta_{m,m_0}\delta_{n,n_0}, \tag{2}$$

where $(\cdot)^*$ denotes conjugate operation of a complex-valued number. $\delta_{m,m_0} = 1$ if $m = m_0$, and $\delta_{m,m_0} = 0$ if $m \neq m_0$. $\Re\{\cdot\}$ stands for the real part of a complex-valued number. Due to the fact that, the orthogonality condition of FBMC/OQAM only holds in the real field, imaginary-valued interference occurs between the transmitted real-valued symbols. For simplicity, the imaginary interference factor is defined as

$$\zeta_{m,n}^{m_0,n_0} = \sum_{k=-\infty}^{\infty} g_{m,n}[k]g^*_{m_0,n_0}[k], \tag{3}$$

where $\zeta_{m,n}^{m_0,n_0} = 1$ if $(m,n) = (m_0,n_0)$, and $\zeta_{m,n}^{m_0,n_0}$ is an imaginary value if $(m,n) \neq (m_0,n_0)$, which indicates the interference to the symbol at the time-frequency position $(m_0,n_)$ from the symbol at the time-frequency position (m,n).

Assume a distortion-free channel, i.e., the received signal $r[k] = s[k]$. Then, the demodulation of the received signal is obtained as

$$\begin{aligned}\hat{a}_{m,n} &= \sum_{k=-\infty}^{\infty} r[k]g\left[k - n\frac{M}{2}\right] e^{-j2\pi mk/M} e^{-j\pi(m+n)/2} \\ &= a_{m,n} + ja^c_{m,n},\end{aligned} \tag{4}$$

where $ja^c_{m,n}$ is the imaginary interference mainly from neighboring symbols of $a_{m,n}$ [15], i.e., .

$$ja^c_{m,n} = \sum_{\Omega^*(1,1)}\sum a_{m,n}\zeta_{m,n}^{m_0,n_0}, \tag{5}$$

where $\Omega^*(p,q)$ denotes the neighborhood $\{(m,n) : |m - m_0| \leq p, |n - n_0| \leq q, (m,n) \neq (m_0,n_0).\}$.

Finally, the transmitted symbols can be recovered by

$$\Re\{\hat{a}_{m,n}\} = a_{m,n}. \tag{6}$$

B. Conventional DFT-based PAPR Reduction Scheme

In this subsection, the conventional DFT-based PAPR reduction scheme [11], [12] is presented briefly in FBMC/OQAM systems, which achieves the PAPR reduction without the cost of high complexity, signal distortion or side information.

Fig. 2 depicts the conventional DFT-based PAPR reduction scheme in FBMC/OQAM systems with $N < M$. Assume $x_{m,n}$ is the transmitted symbols with $0 < m \leq N-1$, the signal after the N-point DFT can be written as

$$X_{m,n} = \frac{1}{\sqrt{N}}\sum_{k=0}^{N-1} x_{k,n}e^{-j2\pi mk/N}, \quad m = 0,1,\cdots,N-1. \tag{7}$$

As presented above, the orthogonality condition of FBMC/OQAM only holds in the real field, and the real and imaginary parts of $X_{m,n}$ are separated and transmitted with a half symbol duration, respectively. Therefore, the real-valued transmitted symbols of FBMC/OQAM modulator are obtained as

$$a_{m,2n} = \Re\{X_{m,n}\} \text{ and } a_{m,2n+1} = \Im\{X_{m,n}\}, \tag{8}$$

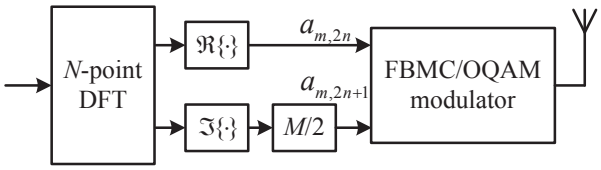

(a) transmitter

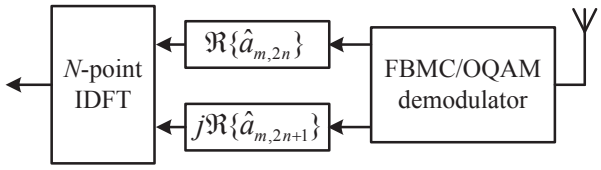

(b) receiver

Fig. 2. Conventional DFT-based PAPR reduction scheme.

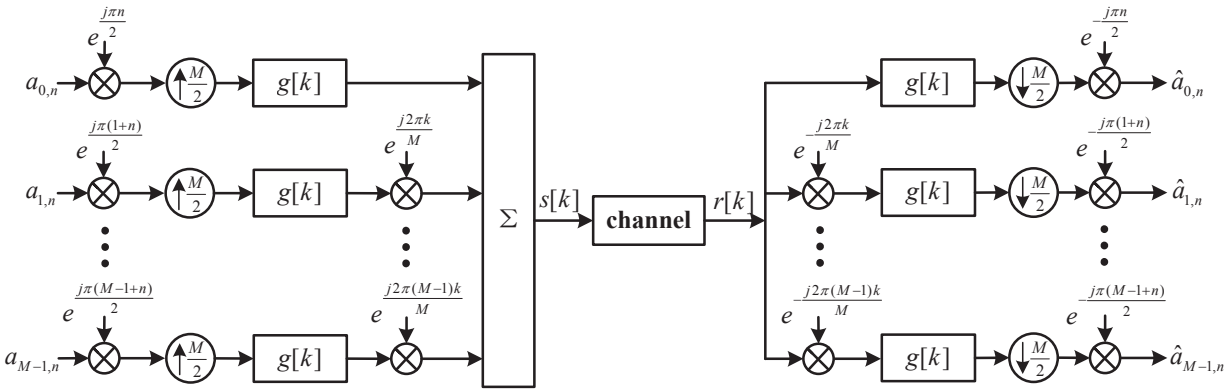

FBMC/OQAM modulator FBMC/OQAM demodulator

Fig. 1. Frame structure for the conventional block-wise Alamouti scheme.

where $\Im\{\cdot\}$ is the imaginary part of a complex-valued number. Note that the interval between $a_{m,2n}$ and $a_{m,2n+1}$ is $T/2$, where T is the symbol duration. Then, the corresponding demodulations, $\hat{a}_{m,2n}$ and $\hat{a}_{m,2n+1}$, at the receiver can be obtained by (4), and the following complex-valued signals are obtained

$$\bar{X}_{m,n} = \hat{a}_{m,2n} + j\hat{a}_{m,2n+1}, \quad m = 0, 1, \cdots, N-1. \tag{9}$$

Finally, after N-point inverse DFT (IDFT), the transmitted symbols can be recovered, i.e.,

$$x_{m,n} = \frac{1}{\sqrt{N}} \sum_{k=0}^{N-1} \bar{X}_{m,n} e^{j2\pi mk/N}, \quad m = 0, 1, \cdots, N-1. \tag{10}$$

The conventional DFT-based scheme reduces the PAPR of FBMC/OQAM systems without the cost of high complexity, signal distortion or side information. However, due to the fact that the real and imaginary parts of the DFT output signals are separated and transmitted, the PAPR reduction is limited.

III. Proposed DFT-based PAPR Reduction Scheme

In this section, we propose a DFT-based scheme for PAPR reduction in FBMC/OQAM systems, based on the concept of block repetition proposed in our previous work [14]. Compared with the conventional DFT-based scheme, the proposed DFT-based scheme can achieve lower PAPR, without the cost of high complexity, signal distortion or side information.

Fig. 3 shows the proposed DFT-based PAPR reduction scheme, in which two blocks are exhibited with an block length of N_s. The second block is the repeated block and symbol reversion is employed. It is worthwhile to note that, compared with the conventional DFT-based scheme, the data rate is maintained in the proposed DFT-based scheme despite of the existence of symbol repetition.

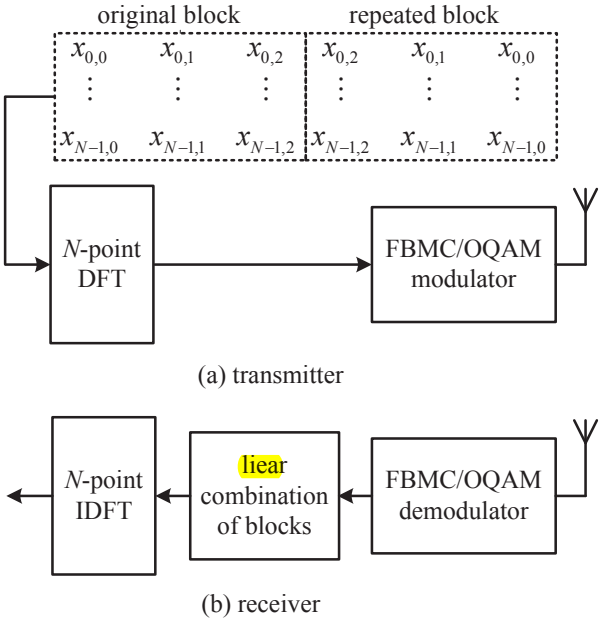

Fig. 3. Proposed DFT-based PAPR reduction scheme.

For the m-th subcarrier, the transmitted complex-valued symbols of original and repeated block are

$$\begin{aligned} &\text{original block:} \quad x_{m,0},\ x_{m,1},\ \cdots, x_{m,N_s-1}, \\ &\text{repeated block:} \quad x_{m,N_s-1},\ \cdots,\ x_{m,1}, x_{m,0}. \end{aligned} \tag{11}$$

The signals after N-point DFT are obtained as

$$\begin{aligned} &\text{original block:} \quad X^o_{m,n} = \frac{1}{\sqrt{N}} \sum_{k=0}^{N-1} x_{k,n} e^{-j2\pi mk/N}, \\ &\text{repeated block:} \quad X^r_{m,N_s-n} = \frac{1}{\sqrt{N}} \sum_{k=0}^{N-1} x_{k,n} e^{-j2\pi mk/N}, \end{aligned} \tag{12}$$

where $m = 0, 1, \cdots, N-1$. It is easily observed that $X^o_{m,n} = X^r_{m,n}$

Different from the conventional DFT-based scheme, the signals after N-point DFT are transmitted directly by the FBMC/OQAM modulator. And then, at the receiver, the demodulated symbols of the FBMC/OQAM demodulator can be obtained according to (4)

$$\begin{aligned} &\text{original block:} \quad \hat{X}^o_{m,n} = X^o_{m,n} + jX^{oc}_{m,n}, \\ &\text{repeated block:} \quad \hat{X}^r_{m,Ns-n} = X^r_{m,n} + jX^{or}_{m,n}, \end{aligned} \tag{13}$$

where $m = 0, 1, \cdots, N-1$. The terms $jX^{oc}_{m,n}$ and $jX^{or}_{m,n}$ are the imaginary interferences, obtained by (5). It can be easily proved that, when symbol reversion as shown in Fig. 2 is employed in the repeated block , the imaginary interferences from the original and repeated blocks can be canceled by a simple linear combination according to the symmetry of the imaginary interference factor [14], i.e.,

$$jX^{oc}_{m,n} + jX^{or}_{m,n} = 0. \tag{14}$$

Therefore, by a simple linear combination, the signal is written as

$$\hat{X}^l_{m,n} = \frac{\hat{X}^o_{m,n} + \hat{X}^r_{m,n}}{2} = X^o_{m,n}. \tag{15}$$

Finally, after N-point IDFT, the transmitted symbols can be recovered, i.e.,

$$x_{m,n} = \frac{1}{\sqrt{N}} \sum_{k=0}^{N-1} \hat{X}^l_{m,n} e^{j2\pi mk/N}, \tag{16}$$

where $m = 0, 1, \cdots, N-1$ and $n = 0, 1, \cdots, N_s - 1$.

In the the proposed DFT-based PAPR reduction method, the output complex-valued signal of the DFT module is directly transmitted, instead of separating and transmitting the real and imaginary parts of the output signal, respectively. The proposed method can provide a solution to the low PAPR without the cost of high complexity, signal distortion or side information. Beside, since the interval of $x_{m,n}$ is $T/2$, the data rate of the proposed scheme is maintained despite of the existence of symbol repetition, compared with the conventional DFT-based PAPR reduction scheme.

IV. Simulation Results

In this section, we provide simulation results of complementary cumulative distribution function (CCDF) and BER, to evaluate the performance of the proposed We consider an FBMC/OQAM system with 2048 subcarriers and isotropic orthogonal transform algorithm (IOTA) filter as prototype filter [15]. Besides, 4QAM is used in simulations and size of DFT is $N = 512$.

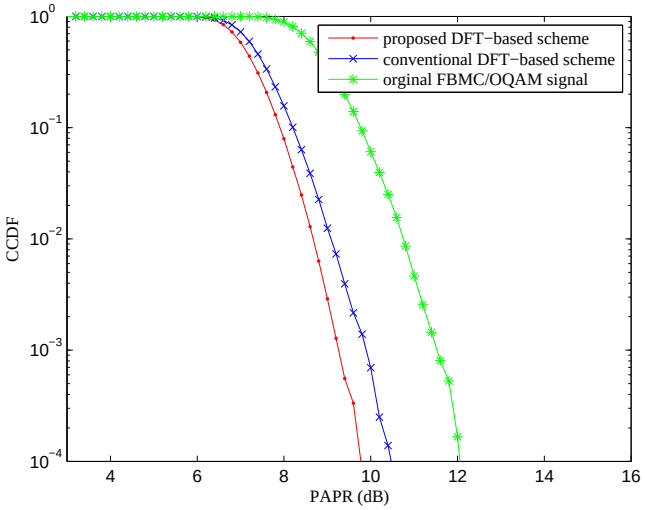

Fig. 4. CCDF of the proposed DFT-based scheme with M=2048 and N=512.

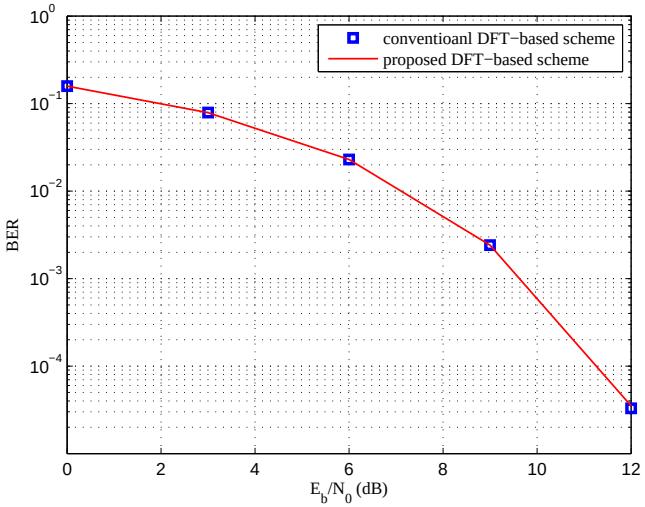

Fig. 5. BER of the proposed DFT-based scheme under AWGN channel.

Fig. 4 and Fig. 5 show the CCDF and BER of the proposed DFT-based scheme in FBMC/OQAM systems, respectively. In simulation, additional white Gaussian noise (AWGN) channel is employed. Simulation results show the proposed DFT-based scheme achieves a better PAPR reduction compared with the conventional DFT-based scheme. Meanwhile, the both of the two schemes exhibit same BER performance under AWGN channel. Therefore, simulation results verify that, the proposed DFT-based scheme is an effective PAPR reduction method in FBMC/OQAM systems, without the cost of high complexity, side information and signal distortion.

V. Conclusion

In this letter, we proposed a DFT-based method for PAPR reduction in FBMC/OQAM systems, based on the concept of block repetition. Compared with the conventional DFT-based PAPR reduction method, the output complex-valued signal of the DFT module would be directly transmitted in the proposed DFT-based PAPR reduction method, instead of separating and transmitting the real and imaginary parts of the output signal, respectively. Simulation results verified that, the proposed DFT-based scheme is an effective PAPR reduction method in FBMC/OQAM systems, without the cost of high complexity, signal distortion or side information.

References

[1] P. Siohan, C. Siclet and N. Lacaille, "Analysis and design of OQAM-OFDM systems based on filterbank theory," *IEEE Transactions on Signal Processing,* vol. 50, no. 5, pp. 1170-1183, May. 2002.

[2] B. Farhang-Boroujeny, "OFDM versus filter bank multicarrier," *IEEE Signal Processing Magazine,* vol. 28, no. 3, pp. 92-112, May. 2011.

[3] D. Qu, S. Lu, and T. Jiang, "Multi-block joint optimization for the peak-to-average power ratio reduction of FBMC-OQAM signals," *IEEE Transactions on Signal Processing,* vol. 61, no. 7, pp. 1605-1613, Jan. 2013.

[4] Z. He, L. Zhou, Y. Chen, and X. Ling, "Low-complexity PTS Scheme for PAPR Reduction in FBMC-OQAM Systems", *IEEE Communications Letters,* vol.22, no.11, pp. 2322-2355, Nov. 2018.

[5] G. Cheng, H. Li, B. Dong, and S. Li, "An improved selective mapping method for PAPR reduction in OFDM/OQAM system," *Communications and Network,* vol. 5, no. 3, pp. 53-56, Sep. 2013.

[6] S. S. Krishna Chaitanya Bulusu, H. Shaiek, D. Roviras, and R. Zayani, "Reduction of PAPR for FBMC-OQAM systems using dispersive SLM technique," *International Symposium on Wireless Communication Systems,* pp. 26-29, Aug. 2014.

[7] A. Skrzypczak, J. P. Javaudin, and P. Siohan, "Reduction of the peakto-average power ratio for OFDM-OQAM modulation," *IEEE Vehicular Technology Conference,* pp. 2018-2022, May. 2006.

[8] S. Lu, D. Qu, and Y. He, "Sliding window tone reservation technique for the peak-to-average power ratio reduction of FBMC-OQAM signals," *IEEE Wireless Communications Letters,* vol. 1, no. 4, pp. 268-271, Jul. 2012.

[9] Z. Kollar, L. Varga, and K. Czimer, "Clipping-based iterative PAPR reduction techniques for FBMC," *International OFDM Workshop,* Essen, Germany, pp. 1-12, Aug. 2012.

[10] Z. Kollar, L. Varga, B. Horvath, P. Bakki, and J. Bito, "Evaluation of clipping based iterative PAPR reduction techniques for FBMC systems," *Scientific World Journal,* vol. 2014, Jan. 2014.

[11] T. Ihalainen, A. Viholainen, T. H. Stitz, M. Renfors, and M. Bellanger, "Filter bank based multi-mode multiple access scheme for wireless uplink," *European Signal Processing Conference,* vol. 9. pp. 1354-1358, Aug. 2009.

[12] D. Na and K. Choi, "Low PAPR FBMC," *IEEE Transactions on Wireless Communications,* vol. 17, no. 1, pp.182-193 Jan. 2018.

[13] R. Nissel and Markus. Rupp, "Pruned DFT-spread FBMC: low PAPR, low latency, high spectral efficiency," to appear in *IEEE Transactions on Communications,* 2019.

[14] D. Kong, X. Zheng, and T. Jiang, "Frame repetition: a solution to imaginary interference cancellation in FBMC/OQAM systems," to appear in *IEEE Transactions on Signal Processing,* 2019.

[15] D. Kong, D. Qu, and T. Jiang, "Time domain channel estimation for OQAM-OFDM systems: algorithms and performance bounds," *IEEE Transactions on Signal Processing,* vol. 62, no. 2, pp. 322-330, Jan. 2014.